Supporting Information

A Generalized Model of Cooperative Covalent Polymerization: Connecting the Supramolecular Binding Interactions with the Catalytic Behavior

Hailin Fu,^{1,‡} Ryan Baumgartner,^{2,‡} Ziyuan Song,^{2,‡} Chongyi Chen,² Jianjun Cheng,^{2,*} and Yao Lin^{1,*}
([†]These authors contributed equally: Hailin Fu, Ryan Baumgartner, Ziyuan Song)

¹Department of Chemistry and Polymer Program at the Institute of Materials Science, University of Connecticut, Storrs, CT 06269, USA

²Department of Materials Science and Engineering and Department of Chemistry, University of Illinois at Urbana-Champaign, Urbana, IL 61801, USA

Materials. All reagents and solvents were purchased from MilliporeSigma (St. Louis, MO, USA) and used as received unless otherwise specified. γ-Benzyl-_L-glutamic acid was purchased from Chem-Impex (Wood Dale, IL, USA). Deuterated dichloromethane (DCM) was purchased from Cambridge Isotope Laboratories, Inc. (Tewksbury, MA, USA). DCM and deuterated DCM were stored over 3 Å molecular sieves in a freezer inside the glovebox. γ-Benzyl-_L-glutamate *N*-carboxyanhydride (BLG-NCA) was synthesized and purified according to literature procedures.^{R1-R3}

Instruments and Characterization Methods. Proton nuclear magnetic resonance (NMR) spectra were recorded on a Varian U500, VXR500, or VNS750NB spectrometer. Chemical shifts (δ) were reported in ppm and referenced to the residual protons in the deuterated solvents. MestReNova software (version 8.1.1, Mestrelab Research, Escondido, CA, USA) was used for all NMR analysis. Fourier transform infrared (FTIR) spectra were collected using a Spectrum 100 spectrometer (PerkinElmer, Santa Clara, CA, USA) in a KBr or ZnSe sealed liquid cell (SL-3 Model, pathlength = 0.1 mm, International Crystal Laboratories, Garfield, NJ, USA). Gel Permeation Chromatography (GPC) was performed on a system equipped with an isocratic pump (1200 or 1260 Infinity II, Agilent Technologies, Inc., Santa Clara, CA, USA), a multi-angle static light scattering (MALS) detector (DAWN HELEOS or DAWN HELEOS-II, Wyatt Technology, Santa Barbara, CA, USA), and a differential refractometer (dRI) detector (Optilab rEX or Optilab T-rEX, Wyatt Technology, Santa Barbara, CA, USA). The detection wavelength of HELEOS was set at 658 nm. Separations were performed using serially connected size exclusion columns (five Phenogel columns, 10² Å, 10³ Å, 10⁴ Å, 10⁵ Å, 10⁶ Å, 5 μm, 300 × 7.8 mm, Phenomenex, Torrance, CA, USA or three PLgel MIXED-B columns, 10 μm, 7.5 × 300 mm, Agilent, Santa Clara, CA, USA) at 60 or 40 °C. The mobile phase consisted of DMF containing LiBr (0.1 M) at a flow rate of 1.0 or 0.7 mL min⁻¹. The MALS detector was calibrated using pure

toluene and can be used for the determination of the absolute molecular weights (MWs). The MWs of polymers were determined using ASTRA software (version 6.1.1.17 or 7.1.3.15, Wyatt Technology, Santa Barbara, CA, USA) and calculated from dn/dc values assuming 100% mass recovery.

Polymerization kinetics. For the polymerization initiated by the diaminoalkane and brush-like macroinitiator, the polymerization kinetics was monitored by quantifying the decrease in the absorbance at 1793 cm⁻¹ (*i.e.*, absorbance of anhydride groups of NCA monomer). For the polymerization initiated by n-hexylamine, the polymerization kinetics was monitored by quantifying the decrease in the NMR signal at δ = 6.4-7.1 ppm (*i.e.*, ring N–H signal of NCA monomer).

In a typical experiment to monitor the polymerization kinetics, BLG-NCA was dissolved in DCM or deuterated DCM in a glovebox, followed by the addition of the solution of initiators to the desired [M]₀ and [M]₀/[I]₀. The resulting solution was transferred into the FTIR liquid cell or the NMR tube, and the FTIR or NMR spectrum was monitored at different time intervals until full conversion. For the brush polymerization system, silanized vials were used for the preparation and the solution was transferred inside the glovebox, mainly due to the moisture-sensitivity of the trimethylsilyl initiating group.

GPC characterization of resulting polypeptides. After the complete conversion of NCA monomer, the solvent was removed under vacuum, and the polymer residues were dissolved in DMF containing LiBr (0.1 M). The resulting solution was filtered through PTFE membranes (0.45 μm) and analyzed by GPC. The GPC plots for homo-polypeptides and brush-like polypeptides can be found in our previous published work. R1,R2 The GPC-LS traces for "hinged" polypeptides are shown in Figure S4.

Kinetic modeling. The differential equations were solved numerically using ode15s in Matlab. The rate constants or equilibrium constants were obtained by minimizing the sum of squared errors between the simulated results and the experimental data. In additional to the major variables used in the generalized OMM model (Table 1), some additional variables discussed in the complex reaction mechanisms are listed below for quick references.

Symbol	Property
k_{on}	Adsorption rate constant for the monomer binding to the active chain to form the complex
k_{off}	Desorption rate constant for the noncovalently bound complex between the monomer
	and active chain end
k ₊	First-order forward rate constant for the conversion reaction between 1st and 2nd
	intermediates
k_{-}	First-order backward rate constant for the conversion reaction between 1st and 2nd
	intermediates
K '	Equilibrium constant for forming the second intermediate, $K^{'}=k_{+}/k_{-}$
k_a	Associating rate constant for the binding of a molecular inhibitor to the reactive site of the
	active chain
k_d	Dissociating rate constant of for the noncovalently bound complex between the molecular
	inhibitor and the growing chain end
K' ₂	Binding equilibrium constant for the competing pathway, $K_2'=k_a/k_a,$

Apply the generalized OMM model to the cooperative covalent polymerization in which a competitive side reaction occurs in the accelerating stage. We provide an additional example in which the generalized OMM model can accurately describe the covalent cooperative polymerization with an inhibitive, competing reaction.

$$\begin{split} M_{i}^{*} + M & \xrightarrow{k_{1}} M_{i+1}^{*} & 1 \leq i < s \\ M_{i}^{*} + M & \xrightarrow{k_{on}} M_{i}^{*} - M \xrightarrow{k_{r}} M_{i+1}^{*} & i \geq s \\ M_{i}^{*} + S & \xrightarrow{k_{a}} M_{i}^{*} - S \end{split}$$

In this example, a molecular inhibitor S, which can bind with the reactive site of the active chain M_i^* ($i \ge s$) reversibly with the associating and dissociating rate constants k_a and k_d , respectively. The binding equilibrium constant for the competing reaction K_2' can be noted as $K_2' = k_a/k_d$. By establishing the concentration flux equations from the reaction scheme (Figure S7), we simulated the kinetic profiles of polymerization (Figure S8a, circles) and the molecular weight distributions of resulting polymers (Figure S8b, solid lines) by numerical method, using an identical set of parameters but initiated from different M_0 . The overall reaction kinetics slow down due to the inhibitive, side reaction. To examine the applicability of the generalized OMM model on this complex mechanism, the kinetic profiles in Figure S8a (circles) were fitted with the generalized OMM model, in which K_M and k_{cat} were used, and the fitted parameters were subsequently used to calculate the MWDs. We found that, in most of cases, the generalized OMM model is a good approximation for the cooperative covalent polymerization with a hypothesized side reaction. Figure S8c shows how the fitted K_M and k_{cat} are related with K_D and k_r used in the simulation of kinetic profiles, respectively, when K_2' varies by a few orders in magnitude.

By applying the steady state assumption for the reversible reactions, we can extract the apparent dissociation equilibrium constant (K_M) and the apparent turnover number (k_{cat}) for the covalent cooperative polymerization with a parallel, inhibitive reaction. It is easy to find that the apparent rate constant in the second stage can be written as:

$$k_{2}' = \frac{k_{r}}{(K_{D} + \frac{k_{r}}{k_{ov}})(1 + K_{2}'S) + M}$$
(S1)

By comparing the apparent propagation rate constant with the form of Michaelis-Menten equation, the analytic equation of K'_{M} and k'_{cat} are derived as:

$$K_M = (K_D + \frac{k_r}{k_{on}})(1 + K_2'S)$$
 (S2)

$$k_{cat} = k_r \tag{S3}$$

For small k_r ,

$$K_{M} \approx K_{D}(1 + K_{2}'S) \tag{S4}$$

Figure S8c show that the prediction from the equations (in solid lines) is in good agreement with the fitting results obtained numerically at individual values of $K_2^{'}$.

$$\begin{split} P_{1}(t) &= \sum_{i=s}^{\infty} M_{i}(t) \\ P_{2}(t) &= \sum_{i=s}^{\infty} (M_{i} - M)(t) \\ \frac{dM(t)}{dt} &= -k_{1}M(t)(I_{0} - P_{1}(t) - P_{2}(t)) - k_{on}M(t)P_{1}(t) + k_{off}P_{2}(t) \\ \frac{dP_{1}(t)}{dt} &= k_{1}M(t)M_{s-1}(t) - k_{on}M(t)P_{1}(t) + (k_{off} + k_{r})P_{2}(t) \\ \frac{dP_{2}(t)}{dt} &= k_{on}M(t)P_{1}(t) - (k_{off} + k_{r})P_{2}(t) \\ \frac{dM_{1}(t)}{dt} &= -k_{1}M(t)M_{1}(t) \\ \frac{dM_{i}(t)}{dt} &= k_{1}M(t)(M_{i-1}(t) - M_{i}(t)) \qquad 1 < i < s \end{split}$$

Figure S1. The concentration-flux kinetic equations for the two-stage covalent cooperative model incorporated with the reversible adsorption and desorption of monomers. As we usually assume $M_1(0) = I_0$ for fast initiation reaction, the initiation step is omitted here for clarity. P_1 , and P_2 are the number concentration of the actively growing chains (M_i^*) and the active intermediates $(M_i^* - M)$, respectively.

$$\mu = \frac{M(t)}{M_0}$$

$$\mu_i = \frac{M_i(t)}{M_0}$$

$$p = \frac{P(t)}{M_0}$$

$$\tau = k_1 M_0 t$$

$$DP^* = \frac{M_0}{I_0}$$

$$\frac{d\mu}{d\tau} = -\mu \left(\frac{1}{DP^*} - p\right) - \frac{k_{cat} \mu p}{k_1 (K_M + \mu M_0)}$$

$$\frac{dp}{d\tau} = \mu \mu_{s-1}$$

$$\frac{d\mu_1}{d\tau} = -\mu \mu_1$$

$$\frac{d\mu_i}{d\tau} = \mu (\mu_{i-1} - \mu_i) \qquad 1 < i < s$$

Figure S2. Dimensionless form of the kinetic equations used for the OMM model. The equation with the presence of M_0 in the right side is highlighted in a red box.

(a) (b)

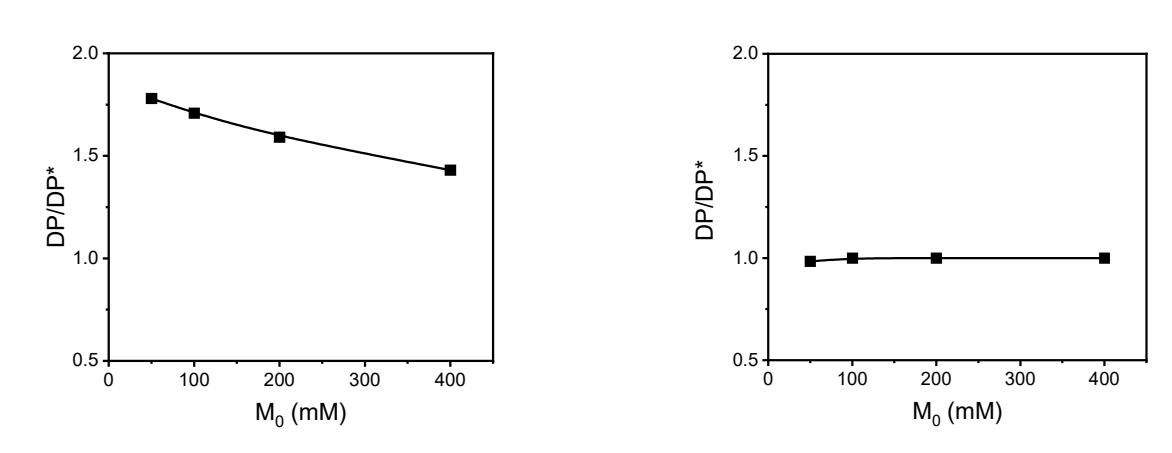


Figure S3. (a) Compare the DP of the resulting polymers with M_0/I_0 (DP*) based on the four kinetic curves in Figure 2c. (b) Compare the DP of the resulting polymers with M_0/I_0 (DP*) based on the four kinetic curves in Figure 2d.

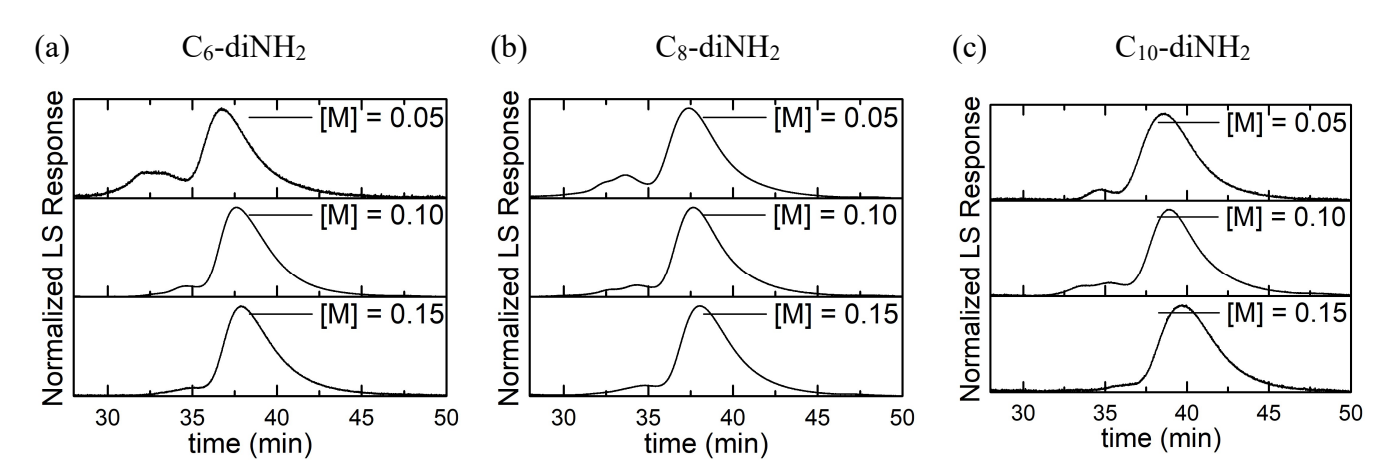


Figure S4. GPC LS traces of "hinged" polypeptides using C_6 -diNH₂ (a), C_8 -diNH₂ (b) and C_{10} -diNH₂ (c) as initiators ($M_0 = 0.05, 0.10, 0.15 \text{ M}, M_0/I_0 = 50$).

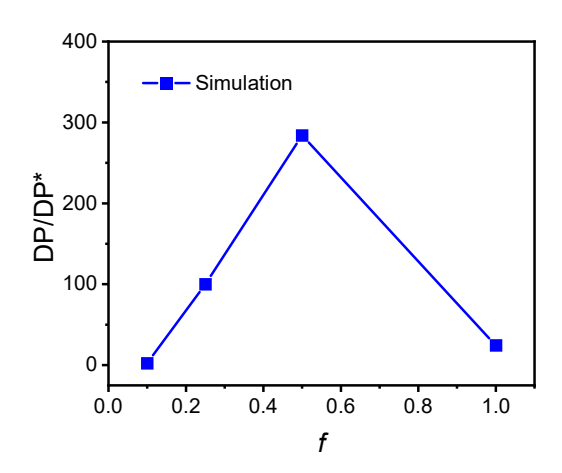


Figure S5. DP of the brush-like polypeptides calculated from the phenomenological model without considering reversible adsorption of monomers (Ref. S2). The original model would predict DP/DP* values significantly deviating from the GPC results.

$$M_{i}^{*} + M \xrightarrow{k_{1}} M_{i+1}^{*} \qquad 1 \leq i < s$$

$$M_{i}^{*} + M \xrightarrow{k_{om}} M_{i}^{*} - M \xrightarrow{k_{+}} M_{i}^{**} - M \xrightarrow{k_{r}} M_{i+1}^{*} \quad i \geq s$$

$$P_{1}(t) = \sum_{l=s}^{\infty} M_{i}(t)$$

$$P_{2}(t) = \sum_{l=s}^{\infty} (M_{i}^{*} - M)(t)$$

$$P_{3}(t) = \sum_{l=s}^{\infty} (M_{i}^{**} - M)(t)$$

$$\frac{dM(t)}{dt} = -k_{1}M(t)(I_{0} - P_{1}(t) - P_{2}(t) - P_{3}(t)) - k_{on}M(t)P_{1}(t) + k_{off}P_{2}(t)$$

$$\frac{dP_{1}(t)}{dt} = k_{1}M(t)M_{s-1}(t) - k_{on}M(t)P_{1}(t) + k_{off}P_{2}(t) + k_{r}P_{3}(t)$$

$$\frac{dP_{2}(t)}{dt} = k_{on}M(t)P_{1}(t) - (k_{off} + k_{+})P_{2}(t) + k_{-}P_{3}(t)$$

$$\frac{dP_{3}(t)}{dt} = k_{+}P_{2}(t) - (k_{-} + k_{r})P_{3}(t)$$

$$\frac{dM_{1}(t)}{dt} = -k_{1}M(t)M_{1}(t)$$

$$\frac{dM_{1}(t)}{dt} = k_{1}M(t)(M_{i-1}(t) - M_{i}(t))$$

$$1 < i < s$$

Figure S6. Concentration flux equations for the covalent cooperative model with hypothesized two intermediates.

$$\begin{split} M_{i}^{*} + M & \xrightarrow{k_{aa}} M_{i}^{*} - M \xrightarrow{k_{r}} M_{i+1}^{*} \quad i \geq s \\ M_{i}^{*} + S & \xrightarrow{k_{a}} M_{i}^{*} - S \end{split}$$

$$P_{1}(t) = \sum_{i=s}^{\infty} M_{i}(t)$$

$$P_{2}(t) = \sum_{i=s}^{\infty} (M_{i} - M)(t)$$

$$P_{3}(t) = \sum_{i=s}^{\infty} (M_{i} - S)(t)$$

$$\frac{dM(t)}{dt} = -k_{1}M(t)(I_{0} - P_{1}(t) - P_{2}(t) - P_{3}(t)) - k_{on}M(t)P_{1}(t) + k_{off}P_{2}(t)$$

$$\frac{dP_{1}(t)}{dt} = k_{1}M(t)M_{s-1}(t) - k_{on}M(t)P_{1}(t) + (k_{off} + k_{r})P_{2}(t) - k_{a}S(t)P_{1}(t) + k_{d}P_{3}(t)$$

$$\frac{dP_{2}(t)}{dt} = k_{on}M(t)P_{1}(t) - (k_{off} + k_{r})P_{2}(t)$$

$$\frac{dP_{3}(t)}{dt} = k_{a}S(t)P_{1}(t) - k_{d}P_{3}(t)$$

$$\frac{dS(t)}{dt} = -k_{a}S(t)P_{1}(t) + k_{d}P_{3}(t)$$

$$\frac{dM_{1}(t)}{dt} = -k_{1}M(t)M_{1}(t)$$

$$\frac{dM_{1}(t)}{dt} = k_{1}M(t)(M_{i-1}(t) - M_{i}(t))$$

$$1 < i < s$$

 $1 \le i < s$

 $M_i^* + M \xrightarrow{k_1} M_{i+1}^*$

Figure S7. Concentration flux equations for the covalent cooperative model in which a hypothesized, competitive side-reaction occurs in the accelerating stage.

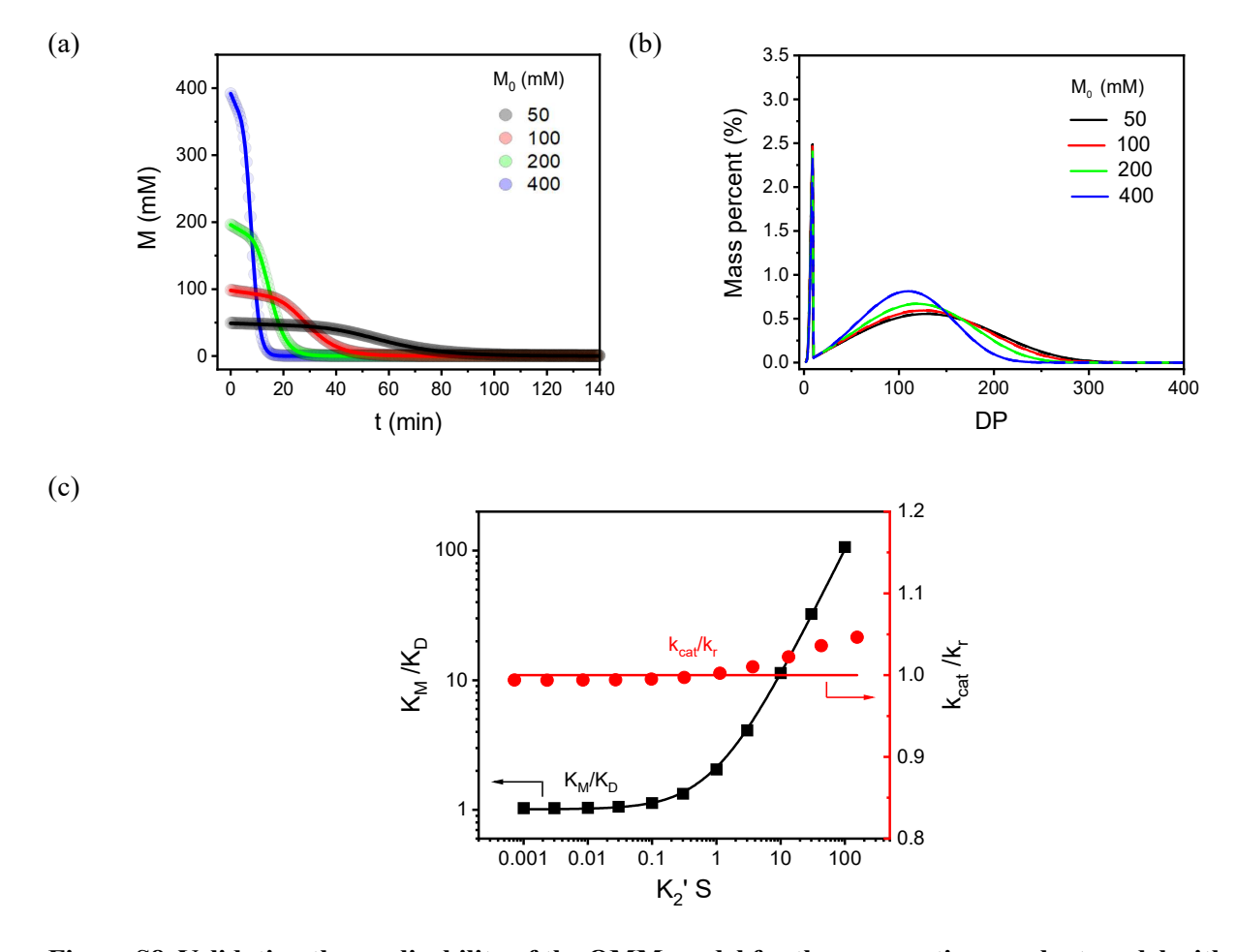


Figure S8. Validating the applicability of the OMM model for the cooperative covalent model with an inhibitive, competing side reaction. (a) Plots of the monomer concentration vs. time (circles) for test cases with s = 10, $M_0/I_0 = 50$, $k_1 = 0.05 \text{ M}^{-1}\text{s}^{-1}$, $k_{on} = 1 \times 10^3 \text{ M}^{-1}\text{ s}^{-1}$, $k_{off} = 1 \times 10^2 \text{ s}^{-1}$, $k_r = 1 \times 10^3 \text{ M}^{-1}\text{ s}^{-1}$, $k_d = 1 \times 10^2 \text{ s}^{-1}$, $k_0 = 1 \times 10^3 \text{ M}^{-1}\text{$

Table S1. Fitting results for the polymerization of homo-polypeptides and comparison with the GPC analysis.

Initiator	M_0 ator M_0/I_0 s		S	k_1	K_D^{-1}	$k_{ m r}$	M_n^1	DP ²	DP^3
1111111111111	(mM)	1110/10	5	$(M^{-1} s^{-1})$	(M^{-1})	(s^{-1})	(kDa)	(GPC)	(calculated)
C ₆ -NH ₂	200	50	10	1.42E-02	6.58E-01	4.2E-01	11.4	52	69
C ₆ -NH ₂	300	50	10	1.69E-02	9.35E-01	4.2E-01	11.7	53	73
C ₆ -NH ₂	400	50	10	2.14E-02	1.07	4.2E-01	12.2	55	69
C ₆ -NH ₂	200	100	10	1.12E-02	1.81E-01	4.2E-01	23.9	109	100
C ₆ -NH ₂	300	100	10	1.25E-02	2.87E-01	4.2E-01	23.2	105	101
C ₆ -NH ₂	400	100	10	1.42E-02	4.06E-01	4.2E-01	23.5	107	102
C ₆ -NH ₂	200	150	10	1.68E-02	1.23E-01	4.2E-01	28.9	131	148
C ₆ -NH ₂	300	150	10	1.14E-02	2.19E-01	4.2E-01	31.4	143	149
C ₆ -NH ₂	400	150	10	1.10E-02	2.89E-01	4.2E-01	32.8	149	148

 $^{^{1}}$ M_{n} is obtained from the GPC results published in our previous work. R1

 $^{^{2}}$ DP = $(M_{n}-M_{I})/M_{0}$, where M_{I} (101.19 Da) and M_{0} (219.24 Da) are the molecular weights of the initiator and the repeating unit in the polypeptide. It's converted from the GPC results.

³ The average DP predicted from the model.

Table S2. Fitting results for the polymerization of "hinged" polypeptides and comparison with GPC analysis.

Initiator	M ₀ (mM)	M_0/I_0	S	k ₁ (M ⁻¹ s ⁻¹)	K_D^{-1} (M-1)	k _r (s ⁻¹)	M _n ¹ (kDa)	DP ² (GPC)	DP ³ (calculated)
C ₆ -diNH ₂	50	50	10	4.4E-02	9.3	1	55.1	125	99-141
C ₆ -diNH ₂	100	50	10	6.6E-02	9.3	1	42.3	96	82-107
C ₆ -diNH ₂	150	50	10	8.9E-02	9.3	1	40.6	92	72-89
C ₈ -diNH ₂	50	50	10	3.0E-02	7.0	1	47.2	107	105-151
C ₈ -diNH ₂	100	50	10	4.3E-02	7.0	1	42.9	98	88-120
C ₈ -diNH ₂	150	50	10	5.8E-02	7.0	1	37.5	85	77-99
C ₁₀ -diNH ₂	50	50	10	2.5E-02	4.4	1	36.6	83	96-134
C_{10} -diNH ₂	100	50	10	3.2E-02	4.4	1	35.0	79	86-115
C ₁₀ -diNH ₂	150	50	10	4.0E-02	4.4	1	30.1	68	78-100

¹ M_n is obtained from the GPC-LS traces shown in Figure S4.

 $^{^2}$ DP = $(M_n-M_I)/2M_0$, where M_I (116.21 Da for C_6 -diNH₂, 144.26 Da for C_8 -diNH₂, 172.32 Da for C_{10} -diNH₂) and M_0 (219.24 Da) are the molecular weights of the initiators and the repeating unit in the polypeptide. The division factor or 2 is used since two helices are linked together by a diamine initiator.

³ The average DP predicted from the model. The lower and upper limit of the calculated DPs are obtained by setting the shortest chain as 8 and 9 repeating units, respectively.

Table S3. Fitting results for the polymerization of "brush" polypeptides and comparison with GPC analysis.

Initiator	Designed f	M ₀ (mM)	M_0/I_0	s	k_1^0 (M ⁻¹ s ⁻¹)	$K_D^{0^{-1}}$ (M ⁻¹)	Fitted f ⁴	k _r (s ⁻¹)	M _n ¹ (kDa)	DP ² (GPC)	DP ³ (calculated)
PNB_{100}	1	50	50	10	1.2E-01	38	1	1	65.5	298	219
PNB ₅₀ -r-PNBPh ₅₀	0.5	50	50	10	1.2E-01	38	0.61	1	51.5	234	250
PNB ₂₅ -r-PNBPh ₇₅	0.25	50	50	10	1.2E-01	38	0.33	1	58.0	263	280
PNB ₁₀ -r-PNBPh ₉₀	0.1	50	50	10	1.2E-01	38	0.12	1	66.9	304	310

¹ M_n is obtained from the GPC results published in our previous work. R2

 $^{^2}$ DP = $(M_n$ - $M_I)/M_0$, where M_I (238.24 Da) and M_0 (219.24 Da) are the molecular weights of the initiator and the repeating unit in the polypeptide. It's converted from the GPC results of the individual helices cut off from the brush polypeptides by ozonolysis. R2

³ The average DP predicted from the OMM model.

⁴ In the global fitting process, f is given a narrow range of variation (±30% of its designed value).

References

R1. Song, Z.; Fu, H.; Baumgartner, R.; Zhu, L.; Shih, K.; Xia, Y.; Zheng, X.; Yin, L.; Chipot, C.; Lin, Y.; Cheng, J. Enzyme-mimetic self-catalyzed polymerization of polypeptides helices. *Nat. Comm.* **2019**, 10, 5470.

R2. Baumgartner, R.; Fu, H.; Song, Z.; Lin, Y.; Cheng, J. Cooperative polymerization of α-helices induced by macromolecular architecture. *Nat. Chem.* **2017**, 9, 614–622.

R3. Chen, C.; Fu, H.; Baumgartner, R.; Song, Z.; Lin, Y.; Cheng, J. Proximity-induced cooperative polymerization in "hinged" helical polypeptides. *J. Am. Chem. Soc.* **2019**, 141, 22, 8680-8683.